

Electrostatic Assembly of Nanoparticles and Biomacromolecules

MURALI SASTRY,^{*,†} MALA RAO,[‡] AND KRISHNA N. GANESH[§]

Materials Chemistry, Biochemical Sciences, and Organic Chemistry (Synthesis) Divisions, National Chemical Laboratory, Pune-411 008, India

Received September 1, 2001

ABSTRACT

The controlled assembly of nanoparticles in thin film form on solid supports, both as monolayers and as superlattice structures, is a problem of considerable topical interest. Among the many interactions used to program the assembly of nanoparticles, electrostatic forces are particularly interesting for many reasons. This Account deals with assembling surface-modified nanoparticles in thin film form using electrostatic interactions at the air–water interface and in thermally evaporated lipid films. The generality of the electrostatic assembly protocol is demonstrated in the immobilization of DNA and proteins in lipid films.

Introduction

The area of nanotechnology is witnessing an unprecedented boom primarily due to the development of improved nanoparticle synthesis protocols and a better understanding of their fundamental physicochemical and optoelectronic properties.¹ One aspect of nanotechnology with a direct impact on commercial application of nanoscale systems is their assembly into superstructures of predefined geometry either in solution or on a solid support. Insofar as formation of monolayer/multilayer thin films of nanoparticles is concerned, the assembly is often carried out by first synthesizing the nanoparticles in solution by the colloidal route and thereafter immobilizing the nanoparticles on various substrates using suitable interactions (the so-called “bottom-up” approach).^{2,3} In this Account, we summarize our research efforts on the assembly of surface-modified nanoparticles

Murali Sastry obtained his masters and doctorate degrees in physics from the Indian Institute of Technology, Madras, in 1987. This was followed by an ICTP postdoctoral stint at the II University of Rome and Sincrotrone Trieste, Italy, in surface physics. Since 1991, he has been at the National Chemical Laboratory, Pune. His research interests include programmed assembly of nanoscale structures, DNA/enzyme–nano/lipid composites, biosynthesis of nanoparticles, and biomineralization.

Mala Rao holds a doctorate in biochemistry from the University of Poona. She has been a visiting scientist at the Swedish Forests Research Products, Stockholm, Purdue University, University of Wisconsin, Madison, and Boston Medical School. Since 1973, she has been at the National Chemical Laboratory, Pune. Her research interests include enzymes from extremophiles, aspartic protease inhibitor, and its interaction with HIV-1 protease.

Krishna Ganesh received his Ph.D. degrees from Delhi University and University of Cambridge (UK) in chemistry. He is currently working in design and synthesis of novel nucleic acid analogues and peptide nucleic acid conjugates for potential applications in diagnostics and therapeutics.

in thin film form using electrostatic interactions. The use of electrostatic forces for assembly enables extension of our protocols to charged biomacromolecules such as proteins and DNA. We discuss in some detail two main methods used by us in the electrostatic assembly of nanoparticles, viz., nanoparticle immobilization at the air–water interface with ionizable Langmuir monolayers and entrapment in thermally evaporated fatty lipid films. Central to our approach is the charging of nanoparticles by suitable ionizable functional groups grafted to the surface of the particles; hence, we deal with this aspect first.

Surface Derivatization of Colloidal Particles

Unlike biomacromolecules such as proteins and DNA that possess an intrinsic electrostatic charge by virtue of amino acid residues and the negatively charged phosphate backbone respectively, charging of inorganic nanoparticles may be effected by attaching ionizable functional groups to the surface. The colloidal route for the synthesis of nanoparticles such as Au, Ag, and CdS is particularly attractive since surface modification may be easily accomplished in solution. It is well known that alkanethiols bind to gold,⁴ silver,⁵ and CdS nanoparticles⁶ via covalent linkage, which thus provides a facile means of modifying the surface of the nanoparticles with specific terminal functional groups. The interesting properties and applications of such monolayer protected clusters (MPCs) have been recently covered by Murray and co-workers.⁷ In our studies, the colloidal particles were synthesized in an aqueous medium; therefore, charging of the particles may be easily accomplished by grafting ionizable carboxylic acid and amine functional groups to the particle surface. Carboxylic acid modification of aqueous gold,⁸ silver,⁹ and CdS¹⁰ nanoparticles was done by chemisorbing monolayers of the bifunctional molecule, 4-carboxythiophenol (4-CTP), on the surface of the nanoparticles (Scheme 1, step A). This process is known to displace surface-bound ions which, in the case of aqueous gold colloids, are known to stabilize the particles. Ionization of the carboxylic acid groups leads to electrostatic stabilization of the particles and a means of extracting from solution and assembling the nanoparticles on oppositely charged solid surfaces. The attractiveness of such a protocol is that simple variation in solution pH would lead to control over degree of ionization of the carboxylic acid/amine functional groups and the ability to modulate electrostatic interactions between the nanoparticles and the immobilizing surface. In a sense, these MPCs would behave like giant ions of variable valency.

During the course of our studies on surface modification of colloidal particles, we have observed that aqueous silver colloidal particles capped with lauric acid molecules

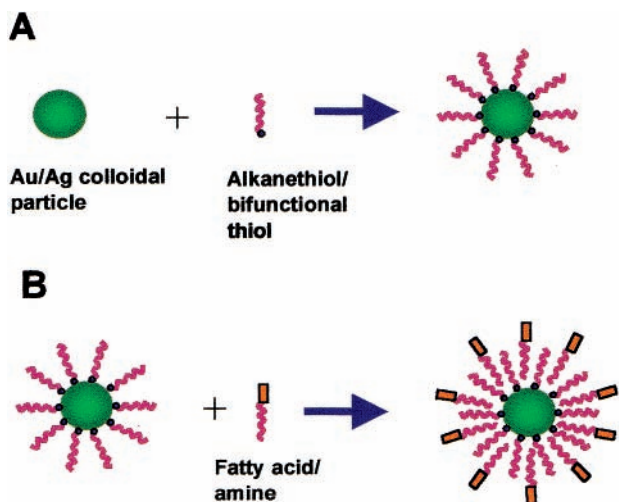
* To whom correspondence should be addressed. Phone: +91 20 5893044. Fax: +91 20 5893952/5893044. E-mail: sastry@ems.ncl.res.in.

[†] Materials Chemistry Division.

[‡] Biochemical Sciences Division.

[§] Organic Chemistry (Synthesis) Division.

Scheme 1. Diagram of Surface Modification of Colloidal Particles: (A) Formation of Primary Monolayer of Alkanethiols/Bifunctional Thiol Molecules and (B) Formation of Interdigitated Secondary Monolayer of Alkylamines/Alkylcarboxylic Acids around the Alkanethiol Primary Monolayer

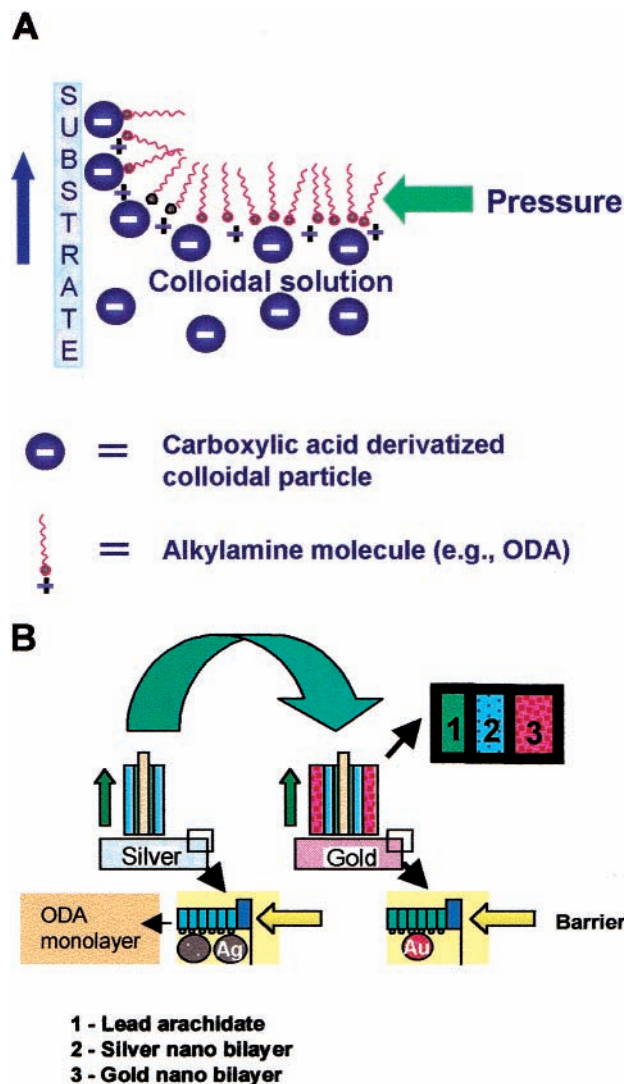


exhibited excellent long-term stability and the ability to bind electrostatically with Langmuir monolayers of fatty amines.¹¹ It was shown that these features were due to formation of interdigitated bilayers of lauric acid molecules on the nanoparticle surface.¹¹ We subsequently developed this strategy to first attach a well-bound alkanethiol monolayer on the silver nanoparticle surface (termed the primary monolayer, step A in Scheme 1), which may then be followed by forming an interdigitated monolayer of an alkylamine/alkylcarboxylic acid (the secondary monolayer, step B in Scheme 1).^{12,13} This protocol for surface modification of nanoparticles without the use of bifunctional molecules has been used in the stabilization and immobilization of the nanoparticles at the air–water interface^{11,12,14} and in thermally evaporated fatty lipid films.¹³ Recently, we have applied this strategy to derivatize gold colloids with biotin functional groups and have followed the prototypical biotin–avidin interaction colorimetrically.¹⁵ Shen, Laibinis, and Hatton have shown that such interdigitated bilayers may be used to stabilize magnetic nanoparticles in solution.¹⁶

Nanoparticle Assembly at the Air–Water Interface

The air–water interface has long been recognized as an excellent medium for the organization of inorganic ions¹⁷ and biomacromolecules such as DNA¹⁸ and proteins¹⁹ as well as nanoparticles.^{20,21} The interested reader is directed to the reviews by Fendler and co-workers on the use of the air–water interface in the assembly of hydrophobized nanoparticles as well as nanoparticles synthesized by chemical reaction of ions bound to Langmuir monolayers.²⁰ Viewing colloidal particles derivatized with carboxylic acid/amine functionality as giant ions, we have developed a strategy for the electrostatic immobilization of nanoparticles of gold,²² silver,^{11,12,23} and CdS¹⁰ with op-

Scheme 2.^a (A) Diagram Showing Electrostatic Immobilization of Carboxylic Acid-Derivatized Colloidal Particles at the Air–Water Interface with Fatty Amine Langmuir Monolayers and Vertical Lifting of the Nanoparticle Monolayers onto Solid Supports by the LB Method and (B) Diagram Illustrating the Assembly of Colloidal Gold and Silver Particles in an Alternating Layer-by-Layer Fashion on Solid Substrates by the LB Technique



^a Reprinted with permission from ref 26. Copyright 2000 Kluwer Academic Publishers.

positively charged Langmuir monolayers at the air–water interface in a manner similar to that adopted for inorganic ions.¹⁷ Scheme 2A illustrates the electrostatic complexation of negatively charged carboxylic acid-derivatized nanoparticles with positively charged fatty amine Langmuir monolayers (for example, octadecylamine (ODA) molecules) at the air–water interface. A powerful feature of this approach is the ability to form multilayer nanoparticle films by sequential immersion of solid supports into the Langmuir monolayer–nanoparticle complexes by the versatile Langmuir–Blodgett (LB) technique.¹⁷ We describe below the formation of multilayer films of silver colloidal particles (derivatized via interdigitated bilayers) by the LB method;¹² this will serve to highlight some of the significant advantages of the electrostatics-based method for nanoparticle assembly.

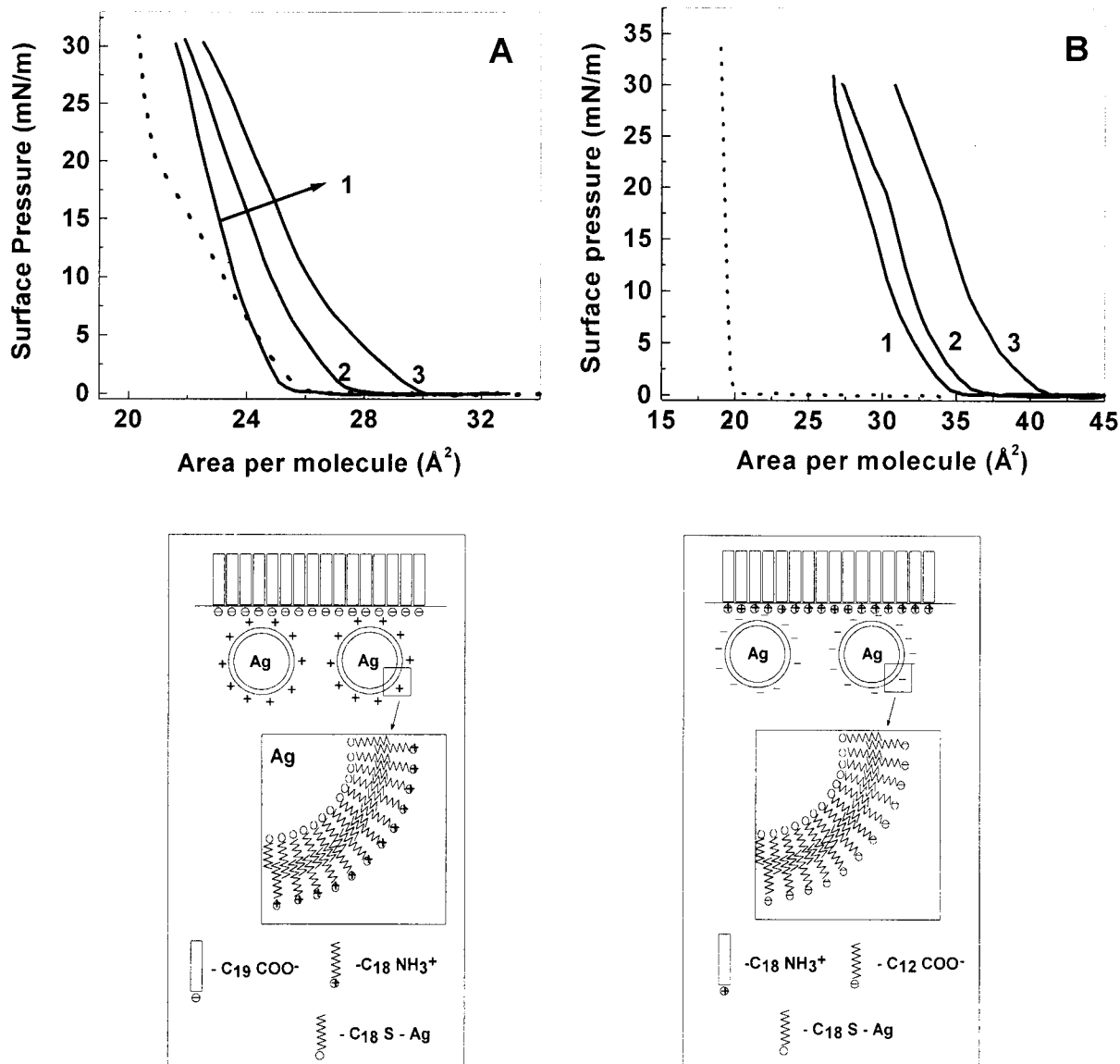


FIGURE 1. (A) π - A isotherms recorded at different times after spreading arachidic acid Langmuir monolayer on the octadecylamine secondary monolayer-capped silver solution (pH 9) as the subphase: 15 min (curve 1), 60 min (curve 2), and 120 min (curve 3). The dashed line corresponds to the π - A isotherm recorded from arachidic acid on pure water at pH 9.¹² (B) π - A isotherms recorded at different times after spreading octadecylamine Langmuir monolayer on the lauric acid secondary monolayer-capped silver solution (pH 9) as the subphase: 15 min (curve 1), 60 min (curve 2), and 120 min (curve 3). The dashed line corresponds to the π - A isotherm recorded from octadecylamine on pure water at pH 9. The accompanying cartoons illustrate the electrostatic complexation of the different surface-modified silver colloidal particles with the oppositely charged Langmuir monolayer and cutaways of the nanoparticle surface showing the interdigitated bilayers.¹²

The real-time complexation of silver colloidal particles (diameter = 70 ± 13 Å) derivatized with carboxylic acid and amine functional groups using interdigitated bilayers (as per the protocol in Scheme 1) with Langmuir monolayers of fatty amine and fatty acids, respectively, may be conveniently studied by monitoring the pressure–area (π - A) isotherms. Figure 1 shows plots of the time dependence of π - A isotherms recorded from a Langmuir monolayer of arachidic acid on amine-derivatized silver particles in the subphase (A) and the corresponding π - A isotherms from the octadecylamine Langmuir monolayer on lauric acid-derivatized colloidal silver solution as the subphase (B). In both cases, it is observed that there is a slow expansion of the monolayer with time, indicating complexation of the silver nanoparticles with the op-

positively charged Langmuir monolayer. Complexation of the fatty amine Langmuir monolayer with the nanoparticle surface-bound carboxylate ions would lead to considerable tilt in the molecules of the Langmuir monolayer (as depicted in Scheme 2A), disruption in the all-trans packing of the hydrocarbon chains, and an increase in the projected surface area of the amine monolayer. Indeed, another study on the kinetics of complexation of carboxylic acid-derivatized silver particles (derivatization accomplished using 4-carboxythiophenol capping molecules) with cationic Langmuir monolayers showed that the complexation was extremely slow, requiring nearly 10–15 h for stabilization of the particle density at the air–water interface.^{23c} The cartoons accompanying the π - A isotherms in Figure 1 illustrate the surface modification

of the silver particles in each of the two cases and electrostatic complexation with the oppositely charged Langmuir monolayer. We caution that these cartoons are highly idealized—the Langmuir monolayer is expected to be much more disordered, as shown in Scheme 2A. The process of immobilization of the silver particles at the air–water interface is not observed to occur under conditions where the Langmuir monolayer is similarly charged¹² or when the Langmuir monolayer is un-ionized.^{23a} Further evidence for the electrostatic nature of binding of the particles with the Langmuir monolayer was provided in another study involving carboxylic acid-derivatized silver particles and Langmuir monolayers consisting of a mixture of fatty amine and fatty alcohols (nonionic) at different relative concentrations.^{23c}

Upon equilibration of the silver particle density at the air–water interface, multilayer films of the nanoparticles were formed on quartz substrates by the versatile LB method and the films subjected to UV–vis spectroscopy analysis.¹² The quartz substrates were rendered hydrophobic prior to silver nanoparticle transfer by depositing three monolayers of lead arachidate on the quartz. This resulted in better quality LB films of the silver nanoparticles. Figure 2 shows the UV–vis spectra recorded from the silver nanoparticle LB films of different thicknesses obtained using Langmuir monolayers of octadecylamine (A, lauric acid secondary monolayers on the silver particle surface) and arachidic acid (B, octadecylamine secondary monolayers on silver). A well-defined absorption band centered at 475 nm is observed in both cases and arises due to excitation of surface plasmon vibrations in the silver nanoparticles.²⁴ The insets of Figure 2A and B show plots of plasmon resonance intensity at 475 nm as a function of number of monolayers of silver particles transferred to the quartz substrates from the octadecylamine and arachidic acid monolayers, respectively. It is seen that there is a linear increase in the plasmon resonance intensity, clearly indicating layer-by-layer transfer of the silver nanoparticles without significant disruption to the nanoparticle density over the range of deposition. This is an important requirement for reliable formation of superlattices of nanoparticles.

The versatility of the LB method lies also in the possibility of growing multilayer films consisting of different layers of amphiphilic molecules²⁵ or nanoparticles²⁶ in any desired sequence by using multiple troughs in the deposition process. This is illustrated schematically for the case of electrostatically immobilized carboxylic acid-derivatized silver and gold nanoparticles at the air–water interface with octadecylamine Langmuir monolayers in Scheme 2B for one cycle of immersion in the two colloidal solutions.²⁶ Sequential immersion of substrates alternatively in two troughs containing silver and gold colloidal solutions results in the transfer of a bilayer of the nanoparticles per dip and formation of a hetero-nanoparticle assembly (Scheme 2B). This process may be extended to films of larger thickness and more complicated nanoparticle sequences, such as the deterministic aperiodic Fibonacci sequence.²⁷

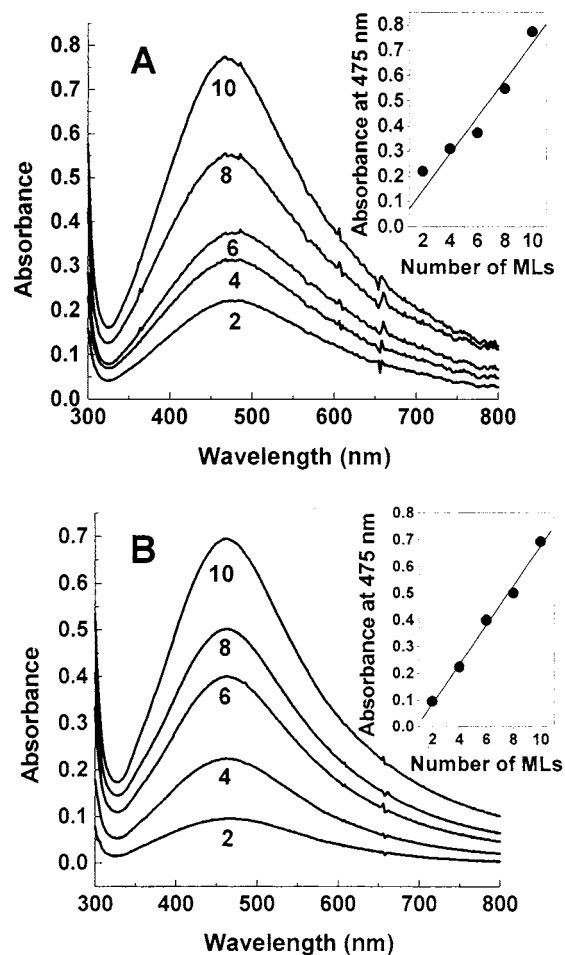


FIGURE 2. (A) UV–vis spectra recorded from octadecylamine LB films as a function of number of monolayers transferred onto hydrophobized quartz substrates from the lauric acid secondary monolayer-capped silver solution. The inset shows a plot of the surface plasmon resonance intensity at 475 nm as a function of number of monolayers in the LB film.¹² (B) UV–vis spectra recorded from arachidic acid LB films as a function of number of monolayers transferred onto hydrophobized quartz substrates from the octadecylamine secondary monolayer-capped silver solution. The inset shows a plot of the surface plasmon resonance intensity at 475 nm as a function of number of monolayers in the LB film.¹²

We have extended the electrostatic air–water immobilization protocol to biomacromolecules such as DNA and demonstrated that hybridization of complementary oligonucleotides (primary base sequence GGAAAAACTTCGTGC) occurs near cationic Langmuir monolayers such as octadecylamine.²⁸ Under physiological pH conditions, the negatively charged phosphate backbone of the oligonucleotides would bind to the cationic fatty amine Langmuir monolayer (step 1 of Figure 3A). Thereafter, injection of the complementary oligonucleotide sequence into the Langmuir trough results in the hybridization of the DNA molecules at the interface (step 2, Figure 3A). The point to note is that DNA hybridization occurs *only at the air–water interface* and not in the bulk solution, which is deionized water and consequently devoid of any salt.²⁸ It is well known that hydrogen bonding between complementary DNA sequences occurs only when the repulsive interactions between the phosphate groups are screened,

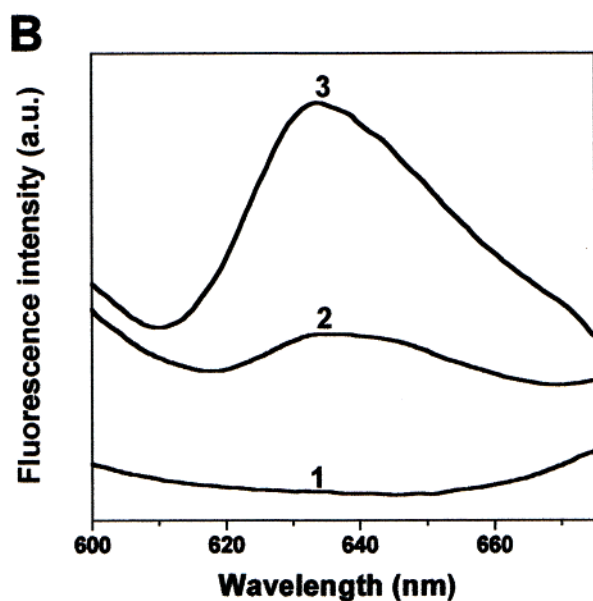
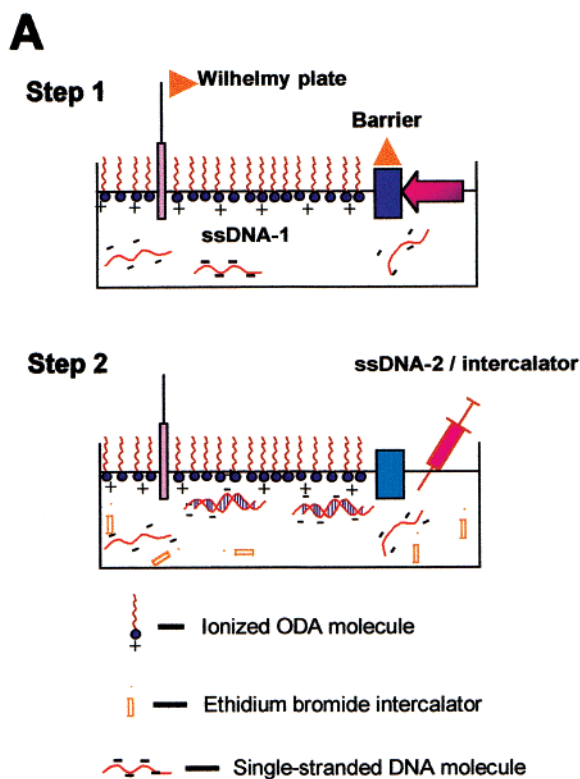


FIGURE 3. (A) Diagram showing the immobilization/hybridization of DNA molecules at the air–water interface with octadecylamine Langmuir monolayers.²⁸ (B) Fluorescence spectra recorded from 19 monolayer LB films of octadecylamine complexed with primary single-stranded DNA followed by a noncomplementary DNA sequence (curve 1), primary sequence followed by the complementary sequence (curve 2), and the LB film with the hybridized DNA structures after further immersion in ethidium bromide solution for 12 h.²⁸

as would occur in the presence of a small amount of salt added to the solution. Thus, the octadecylamine Langmuir monolayer plays the role of counterions, thereby facilitating the DNA hybridization on the surface of water.²⁸ The hybridization of the DNA molecules is conveniently

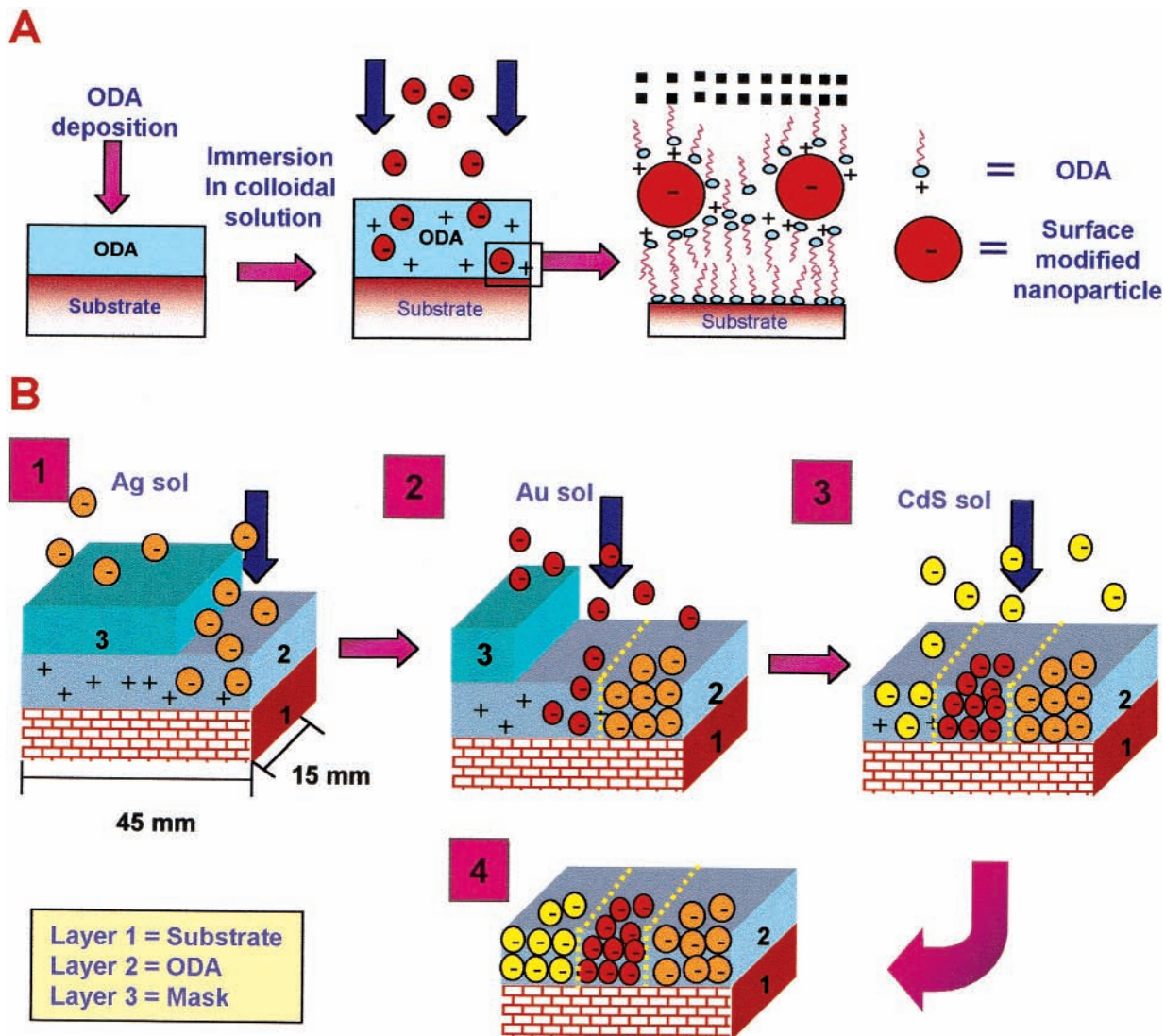
studied by measuring the fluorescence signal from the intercalator, ethidium bromide, which is introduced into the trough along with the complementary DNA molecules.²⁸ Figure 3B shows the fluorescence emission from the intercalator, ethidium bromide (excitation at 460 nm), in 19 monolayer LB films of octadecylamine complexed with the primary DNA sequence followed by a non-complementary DNA sequence (curve 1), octadecylamine complexed with the primary DNA sequence followed by the complementary DNA sequence (curve 2), and the LB film shown as curve 2 after further immersion in ethidium bromide solution for 12 h (curve 3).²⁸ The strong emission observed in films 2 and 3 and the lack of fluorescence in film 1 clearly shows that hybridization of the complementary DNA molecules occurs at the air–water interface and that this process is sensitive to mismatches in the sequence of bases in the single DNA strands. While the hybridization of individual alkylated bases with complementary bases at the air–water interface has been reported,¹⁸ the above study is the first demonstration of hybridization of free oligonucleotides near ionizable Langmuir monolayers.²⁸

Nanoparticle Assembly Using Thermally Evaporated Fatty Lipid Films

In 1996, some of us demonstrated in this laboratory that immersion of thermally evaporated fatty acid films in electrolyte solutions such as $\text{PbCl}_2/\text{CdCl}_2$ resulted in the electrostatic entrapment of the metal cations in the acid matrix, formation of metal salts of the fatty acid, and a consequent spontaneous organization of the film into a *c*-axis-oriented lamellar structure similar to that observed in LB films.²⁹ The use of thermally evaporated fatty lipid films in such an immobilization protocol is exciting for the reason that patterned films may be readily deposited by suitable masking procedures, such patterning not being possible by the LB technique. The entrapment of metal ions followed by their chemical treatment in patterned fatty lipid films has been used to grow organized assemblies of CdS ³⁰ and gold ³¹ nanoparticles as well as hetero-nanoparticle/core–shell nanoparticle structures where their low-temperature alloying behavior was investigated.³²

Following our initial work on the surface modification of colloidal silver and gold particles with carboxylic acid functionality,^{8,9} the electrostatic entrapment of these nanoparticles in thermally evaporated octadecylamine films in a manner similar to that carried out for inorganic ions^{29–32} was attempted. Immersion of fatty amine films in negatively charged silver and gold colloidal solutions resulted in the rapid and visually dramatic appearance of color in the films, demonstrating that the charged nanoparticles were entrapped in the lipid matrix. This simple beaker-based protocol for electrostatic entrapment of nanoparticles is illustrated in Scheme 3A. We have applied this process to entrap silver,^{13,33} gold,³⁴ and CdS nanoparticles³⁵ in thermally evaporated lipid films. The use of electrostatic interactions also enables the entrapment of

Scheme 3. (A) Diagram of Preparation of Nanoparticle–Lipid Composite Films by Electrostatically Controlled Entrapment from Solution^a and (B) Diagram Illustrating the Generation of Spatially Separate, Patterned Hetero-colloidal Particle Assemblies in Thermally Evaporated Octadecylamine Films³⁹



^aThe expected microscopic structure of the nanoparticles within the bilayers is also shown.

charged biomacromolecules such as proteins/enzymes³⁶ and DNA³⁷ from solution in thermally evaporated lipid films.

The entrapment of carboxylic acid-derivatized gold colloidal particles of different sizes (20, 35, and 130 Å) into thermally evaporated octadecylamine films under different pH conditions of the gold colloidal solution was studied using quartz crystal microgravimetry (QCM).^{34b} Figure 4A shows plots of the QCM mass uptake recorded from a 500 Å thick octadecylamine film during immersion in the 130 Å gold colloidal solutions at different pH values. The equilibrium mass uptake is a strong function of the solution pH and can be rationalized in terms of electrostatic interactions between the gold particles and the amine film. At pH 7, the carboxylic acid groups on the nanoparticle surface and the amine groups in the lipid film are fully charged, leading to maximum electrostatic interaction between the two entities. At pH 6, the extent of ionization of the carboxylic acid groups decreases, while

at pH 5.2, the charge on the gold nanoparticles is minimum. At pH 11.2, the gold nanoparticle-bound carboxylic acid groups are fully charged while the amine functionality in the lipid film is less ionized (pK_B of octadecylamine = 10.5). Thus, the electrostatic interactions between the nanoparticles and the lipid matrix may be easily modulated by variation in colloidal solution pH to obtain nanocomposites of varying nanoparticle density.

The inset of Figure 4A shows a plot of the time required for equilibration of nanoparticle density in thin octadecylamine films of 500 Å thickness (estimated from QCM measurements) as a function of gold particle size. It is seen that the equilibrium nanoparticle concentration is achieved much sooner in the case of the smaller gold particles, which implies that the “diffusivity” of the particles is size dependent. The term “diffusivity” has been used in a loose sense to enable semiquantitative comparison of the equilibration times of the different size gold nanoparticles in the lipid matrix.^{33b}

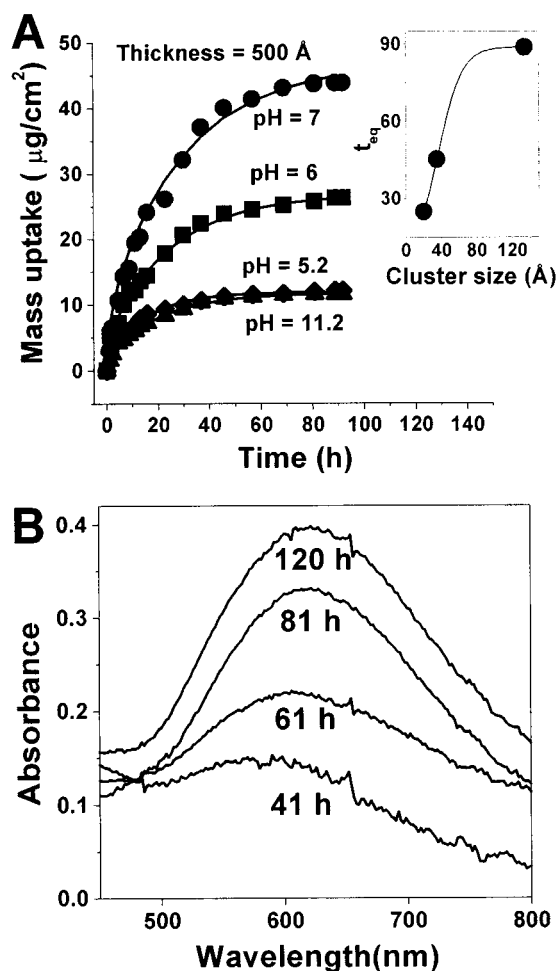


FIGURE 4. (A) QCM mass uptake as a function of time of cluster incorporation for 500 Å thick octadecylamine films immersed in 130 Å diameter gold particle solutions at different pH. The inset shows a plot of the time for equilibration of cluster density in octadecylamine films as a function of cluster size.^{34b} (B) UV-vis spectra recorded in air for 500 Å thick octadecylamine films during immersion in 130 Å size gold colloidal solution (pH 8.5). The time of immersion is indicated next to the respective curves.^{34b}

Figure 4B shows a plot of the UV-vis spectra recorded from a 500 Å thick octadecylamine film during immersion in the 130 Å size colloidal gold solution. The surface plasmon resonance occurs at ca. 610 nm and increases in intensity with time. The increase in the absorption at 610 nm is consistent with the QCM results presented in Figure 4A and provides additional evidence for the presence of gold nanoparticles in the film.

An important challenge in nanoparticle assembly is to realize in-plane patterned nanoparticle structures.³⁸ In a proof-of-concept report, we have shown that patterned hetero-colloidal particle assemblies may be realized by a simple masking procedure and exposure to different colloidal solutions, as illustrated in Scheme 3B.³⁹ In the first step, 33% of the surface of the octadecylamine film is exposed to carboxylic acid-derivatized colloidal silver solution until equilibration of nanoparticle density in the film (step 1). Thereafter, a further 33% of the fresh surface is exposed sequentially to negatively charged gold and CdS nanoparticle solutions respectively (Scheme 3B, steps 2

and 3). This results in three spatially well-defined regions containing different nanoparticles.³⁹ Spot-profile energy dispersive analysis of X-rays in the edge regions suggested little intermixing of the nanoparticles at the edges. Thus, during entrapment of the nanoparticles into the fatty amine matrix, the time-averaged trajectory of the particles is fairly linear and normal to the film surface.³⁹ This method may be extended to more intricately patterned nanoparticle assemblies.

The ability of the lipid films to entrap rigid inorganic nanoparticles larger than the lipid bilayer thickness (Scheme 3A, magnified view of the bilayer) suggests their use as “electrostatic sponges” for the immobilization of more fragile species such as proteins.³⁶ The important question is whether the lipid host is more tolerant of the relatively “soft” and unforgiving nature of the guests. We have studied the electrostatic immobilization of a range of proteins such as the heme proteins cytochrome *c* and hemoglobin^{36d} as well as the enzymes pepsin,^{36a} fungal protease (F-prot),^{36b} and endoglucanase^{36e} in both cationic and anionic lipid films depending on the *pI* of the protein and, in the case of enzymes, the optimum pH of biocatalytic activity. The salient features are illustrated with the example of F-prot immobilization in thermally evaporated fatty acid films.^{36b}

Thermally evaporated arachidic acid films of 250 Å thickness were immersed in F-prot solutions held at different pH values, and the immobilization of the enzyme in the lipid matrix was followed by QCM. Figure 5A shows the QCM mass uptake data as a function of time for three different solution pH values. It is seen that the extent of enzyme loading is highest at pH 6, lowest at pH 9, and intermediate at pH 3. The *pI* of F-prot is 9, and the QCM results may be rationalized in terms of an electrostatic model. At pH 6, the enzyme molecules are fully positively charged while the fatty acid matrix is negatively charged. At pH 3 and 9, the charge on the lipid matrix and the protein molecules respectively is reduced; therefore, the protein loading in the films falls. An interesting feature of the electrostatic immobilization protocol is that, once entrapped, the electrostatic interactions between the host and guest can be modulated (reduced) and the guest enzyme molecules can be pumped out into solution. The inset of Figure 5A shows the release of F-prot molecules from the arachidic acid matrix during immersion in water at pH 3.^{36b} We would like to mention here that immersion of a fully loaded arachidic acid–F-prot biocomposite film in water at pH 6 resulted in a negligible loss of protein from the composite film. This clearly shows that the loss of protein during immersion in water at low pH is due to electrostatic considerations and not due to protein instability in the matrix.

Figure 5B shows the Fourier transform infrared (FTIR) spectra recorded from the as-deposited arachidic acid film (curve 1), the arachidic acid–F-prot bioconjugate film (curve 2), the bioconjugate film after biocatalytic activity measurements (curve 3), and the bioconjugate film after aging in air for 5 days at room temperature (curve 4). Feature *c* at 1700 cm⁻¹ corresponds to the carbonyl stretch

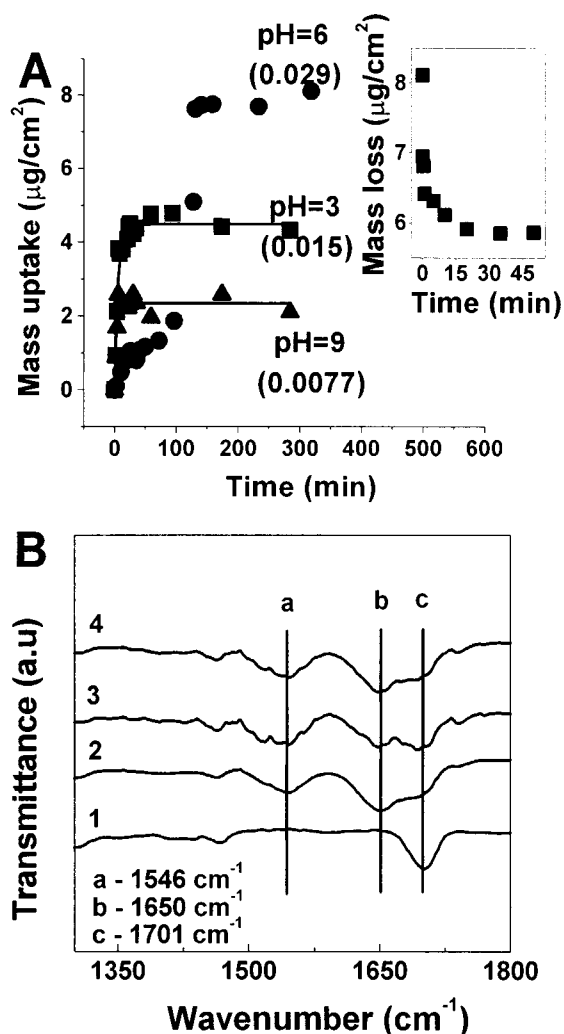


FIGURE 5. (A) QCM kinetics of incorporation of F-prot in arachidic acid films during immersion in 10^{-6} M F-prot solutions at different pH values (pH indicated next to the curves). The equilibrium F-prot–arachidic acid molar ratio values are also indicated.^{36b} The inset shows a plot of the F-prot–arachidic acid bioconjugate film mass loss during immersion in water at pH 3. (B) FTIR spectra of the as-deposited arachidic acid film (curve 1), the F-prot–arachidic acid bioconjugate film (curve 2), the bioconjugate film after biocatalytic activity measurements (curve 3), and the bioconjugate film after aging in air at room temperature for 5 days (curve 4).^{36b}

modes of the carboxylic acid groups in the acid matrix, while the absorption band features a and b at 1546 and 1650 cm^{-1} are the amide II and I bands, respectively. The amide I and II bands clearly occur only in the bioconjugate film (curves 2 and 3) and indicate that the secondary structure of the enzyme molecules is retained on entrapment in the acid matrix.^{36b} There is little deterioration of the bioconjugate film with aging (curve 4).

The ultimate test of enzyme tertiary structure integrity is retention of biological activity. The catalytic activity of the arachidic acid–F-prot film was estimated by standard procedures^{36b} and compared with that of the free enzyme in solution. Specific activities could be estimated for the bioconjugate film since the amount of enzyme could be accurately determined from QCM measurements.^{36b} The specific activity of the bioconjugate film (61.8 ± 4.9 units/

mg) compared favorably with that of the free enzyme in solution (65 units/mg).^{36b} Furthermore, the bioconjugate films could be used repeatedly in biocatalytic reactions and resulted in improved temporal stability of the entrapped enzyme.^{36b} We believe the use of a soft matrix such as that provided by thermally evaporated lipid films in the immobilization of enzymes has immense potential with significant advantages over other currently used immobilization methods such as the sol–gel route (see refs 36b and 36e for a discussion), and we are currently investigating entrapment of structurally unstable proteins as well as means of overcoming “mass-transport” limitations. Recently, we have shown that DNA entrapment and hybridization can be accomplished in such lipid films with important implications in gene sequencing, etc.³⁷

In this Account, we have attempted to show how electrostatic interactions may be used in the formation of lipid–nanoparticle conjugate materials of variable composition and topological structure both at the air–water interface and in thermally evaporated lipid films. The use of thermally evaporated lipid films for extracting nanoparticles/biomacromolecules from solution enables easy patterning of the films and has raised a number of issues of a fundamental nature. Potential applications of enzyme–lipid conjugate materials in sensors, patterned DNA–lipid films in gene sequencing, and inorganic nanoparticle–lipid films as supported catalysts are being pursued.

M.S. acknowledges the contributions of his former and present Ph.D. students, particularly Mr. Anand Gole and Ms. Vidya Ramakrishnan. M.S. thanks the Council of Scientific and Industrial Research, Government of India, for financial assistance through a special “Young Scientist” award grant (1996–2000).

References

- (1) Schmid, G., Ed. *Clusters and Colloids*; VCH: Weinheim, 1994.
- (2) Fendler, J. H. Self-assembled nanostructured materials. *Chem. Mater.* **1996**, *8*, 1616–1624.
- (3) Shipway, A. N.; Katz, E.; Willner, I. Nanoparticle arrays on surfaces for electronic, optical, and sensor applications. *ChemPhysChem* **2000**, *1*, 18–52.
- (4) Brust, M.; Walker, M.; Bethell, D.; Schiffrin, D. J.; Whyman, R. Synthesis of thiol-derivatized gold nanoparticles in a two-phase liquid–liquid system. *J. Chem. Soc., Chem. Commun.* **1994**, 801–802.
- (5) Malinsky, M. D.; Kelly, K. L.; Schatz, G. C.; Van Duyne, R. P. Chain length dependence and sensing capabilities of the localized surface plasmon resonance of silver nanoparticles chemically modified with alkanethiol self-assembled monolayers. *J. Am. Chem. Soc.* **2001**, *123*, 1471–1482.
- (6) Colvin, V. L.; Goldstein, N.; Alivisatos, A. P. Semiconductor nanocrystals covalently bound to metal surfaces with self-assembled monolayers. *J. Am. Chem. Soc.* **1992**, *114*, 5221–5230.
- (7) Templeton, A. C.; Wuelfing, W. P.; Murray, R. W. Monolayer-protected cluster molecules. *Acc. Chem. Res.* **2000**, *33*, 27–36 and references therein.
- (8) Mayya, K. S.; Patil, V.; Sastry, M. On the stability of carboxylic acid derivatized gold colloidal particles: the role of colloidal solution pH studied by optical absorption spectroscopy. *Langmuir* **1997**, *13*, 3944–3947.
- (9) Sastry, M.; Mayya, K. S.; Bandyopadhyay, K. pH dependent changes in the optical properties of carboxylic acid derivatized silver colloidal particles. *Colloids Surf. A* **1997**, *127*, 221–228.
- (10) Mayya, K. S.; Patil, V.; Kumar, P. M.; Sastry, M. On the deposition of Langmuir–Blodgett films of Q-state CdS nanoparticles through electrostatic immobilization at the air–water interface. *Thin Solid Films* **1998**, *312*, 300–305.

- (11) Patil, V.; Mayya, K. S.; Pradhan, S. D.; Sastry, M. Evidence for novel interdigitated bilayer formation of fatty acids during three-dimensional self-assembly on silver colloidal particles. *J. Am. Chem. Soc.* **1997**, *119*, 9281–9282.
- (12) Sastry, M.; Mayya, K. S.; Patil, V. Facile surface modification of colloidal particles using bilayer surfactant assemblies: a new strategy for electrostatic complexation in Langmuir–Blodgett films. *Langmuir* **1998**, *14*, 5921–5928.
- (13) Patil, V.; Mayya, K. S.; Sastry, M. Surface derivatization of colloidal silver particles using interdigitated bilayers: a novel strategy for electrostatic immobilization of colloidal particles in thermally evaporated fatty acid/fatty amine films. *Langmuir* **1998**, *14*, 2707–2711.
- (14) Damle, C.; Gole, A.; Sastry, M. Multilayer Langmuir–Blodgett assemblies of CdS nanoparticles by organization at the air–water interface. *J. Mater. Chem.* **2000**, *10*, 1389–1393.
- (15) Lala, N.; Sastry, M. Biotinylation of colloidal gold particles by a novel interdigitation process and colorimetric detection of the biotin–avidin molecular recognition process. *Colloids Surf. A*, in press.
- (16) Shen, L.; Laibinis, P. E.; Hatton, T. A. Bilayer surfactant stabilized magnetic fluids: synthesis and interactions at interfaces. *Langmuir* **1999**, *15*, 447–453.
- (17) Ulman, A. *Introduction to ultrathin organic films: from Langmuir–Blodgett to self-assembly*; Academic Press: San Diego, 1991.
- (18) Ebara, Y.; Mizutani, K.; Okahata, Y. DNA hybridization at the air–water interface. *Langmuir* **2000**, *16*, 2416–2418.
- (19) Boussaad, A.; Dziri, L.; Arechabaleta, N. J.; Tao, N. J.; LeBlanc, R. M. Electron-transfer properties of cytochrome c Langmuir–Blodgett films and interactions of cytochrome c with lipids. *Langmuir* **1998**, *14*, 6215–6219.
- (20) Fendler, J. H.; Meldrum, F. C. The colloid chemical approach to nanostructured materials. *Adv. Mater.* **1995**, *7*, 607–632 and references therein.
- (21) (a) Sastry, M.; Patil, V.; Mayya, K. S.; Paranjape, D. V.; Singh, P.; Sainkar, S. R. Organization of polymer-capped platinum colloidal particles at the air–water interface. *Thin Solid Films* **1998**, *324*, 239–244. (b) Sastry, M.; Gole, A.; Patil, V. Lamellar Langmuir–Blodgett films of hydrophobized gold nanoparticles by organization at the air–water interface. *Thin Solid Films* **2001**, *384*, 125–131.
- (22) (a) Mayya, K. S.; Patil, V.; Sastry, M. Lamellar multilayer gold cluster films deposited by the Langmuir–Blodgett technique. *Langmuir* **1997**, *13*, 2575–2577. (b) Mayya, K. S.; Patil, V.; Sastry, M. Influence of colloidal subphase pH on the deposition of multilayer Langmuir–Blodgett films of gold clusters. *J. Chem. Soc., Faraday Trans.* **1997**, *93*, 3377–3381.
- (23) (a) Sastry, M.; Mayya, K. S.; Patil, V.; Paranjape, D. V.; Hegde, S. G. Langmuir–Blodgett films of carboxylic acid derivatized silver colloidal particles: role of subphase pH on degree of cluster incorporation. *J. Phys. Chem. B* **1997**, *101*, 4954–4958. (b) Mayya, K. S.; Sastry, M. A study of the partitioning of colloidal particles based on their size during electrostatic immobilization at the air–water interface using fatty amine monolayers. *J. Phys. Chem. B* **1997**, *101*, 9790–9793. (c) Mayya, K. S.; Sastry, M. Electrostatic complexation of carboxylic acid derivatized silver colloidal particles with fatty amine Langmuir monolayers. Role of neutral spacer molecules in the monolayer. *Langmuir* **1998**, *14*, 74–78.
- (24) Henglein, A. Metal particles in solution: “microelectrode” reaction, chemisorption, composite metal particles and the atom-to-metal transition. *J. Phys. Chem.* **1993**, *97*, 5457–5471. These plasmon excitations are responsible for the striking colors of silver (bright yellow) and gold (pink to ruby red) colloidal solutions.
- (25) Ganguly, P.; Sastry, M.; Chaudhary, S.; Paranjape, D. V. “Turn-over” of amphiphile molecules in Langmuir–Blodgett films of salts of fatty acids: an X-ray diffraction study. *Langmuir* **1997**, *13*, 6582–6588.
- (26) Sastry, M.; Mayya, K. S. Hetero-colloidal metal particle multilayer films grown using electrostatic interactions at the air–water interface. *J. Nanopart. Res.* **2000**, *2*, 183–190.
- (27) Gellerman, W.; Kohmoto, M.; Sutherland, B.; Taylor, P. C. Localization of light waves in Fibonacci dielectric multilayers. *Phys. Rev. Lett.* **1994**, *72*, 633–636.
- (28) Sastry, M.; Ramakrishnan, V.; Pattarkine, M.; Gole, A.; Ganesh, K. N. Hybridization of DNA by sequential immobilization of oligonucleotides at the air–water interface. *Langmuir* **2000**, *16*, 9142–9146.
- (29) Ganguly, P.; Sastry, M.; Pal, S.; Shashikala, M. N. Spontaneous self-organization and cation exchange in fatty acid films immersed in aqueous media. *Langmuir* **1995**, *11*, 1078–1080.
- (30) Mandal, S.; Damle, C.; Sainkar, S. R.; Sastry, M. Assembly of CdS nanoparticles in patterned structures by a novel ion-entrapment process in thermally evaporated fatty acid films. *J. Nanosci. Nanotechnol.* **2001**, *1*, 281–285.
- (31) Mandal, S.; Sainkar, S. R.; Sastry, M. Electrostatic entrapment of chloroaurate ions in patterned lipid films and the in-situ formation of gold nanoparticles. *Nanotechnology* **2001**, *12*, 358–362.
- (32) (a) Kumar, A.; Damle, C.; Sastry, M. Low-temperature crystalline Ag–Ni alloy formation from silver and nickel nanoparticles entrapped in fatty acid composite films. *Appl. Phys. Lett.* **2001**, *79*, 3314–3316. (b) Damle, C.; Biswas, K.; Sastry, M. Synthesis of Au-core/Pt-shell nanoparticles within thermally evaporated fatty amine films and their low-temperature alloying. *Langmuir* **2001**, *17*, 7156–7159.
- (33) (a) Sastry, M.; Patil, V.; Mayya, K. S. Incorporation of colloidal metal particles in thermally evaporated fatty amine films by selective electrostatic interactions. *Langmuir* **1997**, *13*, 4490–4492. (b) Sastry, M.; Patil, V.; Sainkar, S. R. Electrostatically controlled diffusion of carboxylic acid derivatized silver colloidal particles in thermally evaporated fatty amine films. *J. Phys. Chem. B* **1998**, *102*, 1404–1410. (c) Patil, V.; Sastry, M. Formation of close-packed silver colloid multilayers from electrostatically formed octadecylamine/colloid nanocomposite precursors. *Langmuir* **2000**, *16*, 2207–2212.
- (34) (a) Patil, V.; Sastry, M. Unusual partitioning of clusters based on their size during electrostatically controlled diffusion of carboxylic acid derivatized colloidal particles in thermally evaporated fatty amine films. *Langmuir* **1997**, *13*, 5511–5513. (b) Patil, V.; Malvankar, R. B.; Sastry, M. Role of particle size in individual and competitive diffusion of carboxylic acid derivatized colloidal gold particles in thermally evaporated fatty amine films. *Langmuir* **1999**, *15*, 8197–8206.
- (35) Patil, V.; Sastry, M. Electrostatically controlled diffusion of Q-state CdS nanoparticles in thermally evaporated fatty amine films. *J. Chem. Soc., Faraday Trans.* **1997**, *93*, 4347–4353.
- (36) (a) Gole, A.; Dash, C.; Rao, M.; Sastry, M. Encapsulation and biocatalytic activity of the enzyme pepsin fatty lipid films by selective electrostatic interactions. *J. Chem. Soc., Chem. Commun.* **2000**, 297–298. (b) Gole, A.; Dash, C.; Mandale, A. B.; Rao, M.; Sastry, M. Fabrication, characterization, and enzymatic activity of encapsulated fungal protease-fatty lipid biocomposite films. *Anal. Chem.* **2000**, *72*, 4301–4309. (c) Gole, A.; Sastry, M. A new method for the generation of patterned protein films by encapsulation in arrays of thermally evaporated lipids. *Biotechnol. Bioeng.* **2001**, *74*, 172–178. (d) Gole, A.; Chaudhari, P.; Kaur, J.; Sastry, M. Protein-friendly intercalation of cytochrome c and hemoglobin into thermally evaporated anionic and cationic lipid films: a new approach based on diffusion from solution. *Langmuir* **2001**, *17*, 5646–5656. (e) Gole, A.; Vyas, S.; Sainkar, S. R.; Lachke, A. L.; Sastry, M. Enhanced temperature and pH stability of fatty amine-endoglucanase composites: fabrication, substrate protection and biological activity. *Langmuir* **2001**, *17*, 5964–5970.
- (37) Sastry, M.; Ramakrishnan, V.; Pattarkine, M.; Ganesh, K. N. Studies on the formation of DNA–cationic lipid composite films and DNA hybridization in the composites. *J. Phys. Chem. B* **2001**, *105*, 4409–4414.
- (38) (a) He, H. X.; Zhang, H.; Li, Q. G.; Zhu, T.; Li, S. F. Y.; Liu, Z. F. Fabrication of designed architectures of Au nanoparticles on solid substrate with printed self-assembled monolayers as templates. *Langmuir* **2000**, *16*, 3846–3851. (b) Aizenberg, J.; Braun, P. V.; Wiltzius, P. Patterned colloidal deposition controlled by electrostatic and capillary forces. *Phys. Rev. Lett.* **2000**, *84*, 2997–3000.
- (39) Sastry, M.; Gole, A.; Sainkar, S. R. Formation of patterned, heterocolloidal nanoparticle thin films. *Langmuir* **2000**, *16*, 3553–3556.

AR010094X